



Article

Long-Term SAR Data Analysis for Subsidence Monitoring and Correlation Study at Beijing Capital Airport

Yueze Zheng ^{1,2} , Junhuan Peng ^{1,*}, Chuyu Li ², Xue Chen ³ , Yun Peng ⁴, Xu Ma ¹ and Meng Huang ²

¹ School of Land Science and Technology, China University of Geosciences, 29 Xueyuan Lu, Beijing 100083, China; zheng_cugb@163.com (Y.Z.)

² Beijing Institute of Surveying and Mapping, 15 Yangfangdian Lu, Beijing 100080, China; lichuyu1996@163.com (C.L.); huangmeng121@126.com (M.H.)

³ National Institute of Natural Hazards, Ministry of Emergency Management of China, Beijing 100085, China; chenxue@cugb.edu.cn

⁴ Power China Zhongnan Engineering Corporation Limited, 16 Xiangzhang East Road, Changsha 410014, China; zsertyf@126.com

* Correspondence: pengjunhuan@163.com

Abstract: Land subsidence, resulting from natural or human activities, is a global environmental geological disaster. The Interferometric Synthetic Aperture Radar (InSAR) time-series analysis technique offers high spatial and continuous temporal resolution, providing data and a foundation for investigating regional land subsidence and its evolution mechanism. Beijing Capital International Airport (BCIA) has experienced uneven land subsidence since 1935, together with severe fissures significantly affecting its normal operations. In this study, the time-series InSAR method was successfully applied to monitor the gradual increase in uneven local subsidence and ground fissures activity at BCIA from June 2003 to March 2023. Initially, ENVISAT-ASAR, Cosmo-SkyMed, and Sentinel-1 data were processed by time-series InSAR techniques to generate deformation rate maps and time series for the airport area. Subsequently, a comparison was made between the displacement time series from InSAR and ground leveling measurements to assess the accuracy of InSAR-derived measurements. Through a comprehensive analysis of the distribution characteristics of land subsidence at the airport, a long-standing ground fault was located within the airport was identified. A preliminary discussion on the development status of this ground fissure was carried out based on the visual interpretation of optical images. Lastly, the inducing factors and evolutionary conditions of land subsidence were discussed. This case demonstrates the applicability of InSAR technology in identifying and monitoring geological processes such as land subsidence and ground fissure activities. It provides a scientific approach to exploring and studying the causes and formation mechanisms of land subsidence and ground fissures in the Beijing Capital Airport area.

Keywords: InSAR; ground subsidence; Beijing Capital International Airport; groundwater; fault



Citation: Zheng, Y.; Peng, J.; Li, C.; Chen, X.; Peng, Y.; Ma, X.; Huang, M. Long-Term SAR Data Analysis for Subsidence Monitoring and Correlation Study at Beijing Capital Airport. *Remote Sens.* **2024**, *16*, 445. <https://doi.org/10.3390/rs16030445>

Academic Editor: Michele Saroli

Received: 14 November 2023

Revised: 17 January 2024

Accepted: 20 January 2024

Published: 23 January 2024



Copyright: © 2024 by the authors. Licensee MDPI, Basel, Switzerland. This article is an open access article distributed under the terms and conditions of the Creative Commons Attribution (CC BY) license (<https://creativecommons.org/licenses/by/4.0/>).

1. Introduction

Land subsidence, caused by both natural and anthropogenic processes, is a widespread phenomenon [1,2]. Land subsidence resulting from overexploitation of groundwater aquifers is common worldwide [3–8]. BCIA, the largest civilian airport in Beijing, ranks first in passenger throughput in Asia and second globally, making it one of the busiest international aviation hubs. However, due to historical tectogenesis impacts in Beijing, characterized by complex geological conditions, land subsidence stands as a significant geological hazard, impacting urban infrastructure safety and posing a threat to airport operations [9–11]. Thus, investigating the spatiotemporal characteristics of airport land subsidence is of paramount importance for controlling and mitigating subsidence hazards, safeguarding airport operations, and ensuring public safety.

Traditional methods for land subsidence monitoring, such as leveling instruments and GNSS (Global Navigation Satellite System), are susceptible to terrain and weather-related limitations. Since the 1990s, InSAR has emerged as an effective, rapid, and cost-efficient technology, offering sub-meter spatial resolution and high-frequency revisits for land subsidence measurements [12]. This technology has been widely employed for subsidence monitoring.

Prior research demonstrated that factors such as groundwater levels, aquifer types, and active faults influence land subsidence [13,14]. Given Beijing's high population and limited water resources, intensive groundwater extraction led to noticeable declines in groundwater levels, resulting in ongoing land subsidence and damage to structures and civil infrastructure. Consequently, monitoring land subsidence plays a vital role in controlling and mitigating the impacts of subsidence hazards. Zhou et al. utilized SBAS (Small Baseline Subsets) time-series analysis to investigate surface deformation in the eastern plains of Beijing over five years. They found that subsidence predominantly occurred in aquatic and wetland areas, rice paddies, dry fields, vegetable plots, and agricultural regions [15]. Jie Dong, through multi-platform SAR satellite data, revealed a 30-year history of land subsidence in Beijing, showing a process of minor-rapid-slow-partial uplift over three decades, with subsidence funneling primarily in the city center, northeast, and northern sides. Excessive groundwater extraction was identified as the main cause of subsidence in the Beijing Plain, and the South-to-North Water Diversion Project (SNWDP) mitigated land subsidence [16]. Zhenkai Zhou utilized InSAR to capture fine-scale surface deformation at BCIA, and in conjunction with discrete element modeling, investigated the relationship between runway damage and the formation of ground fissures, influenced by groundwater extraction and active faults [15]. Keren Dai found that the Shunyi-Liangxiang (SL) Fault directly traversed BCIA, causing uneven subsidence and controlling the spatial subsidence pattern to some extent [17]. Gaoming Liang et al. successfully detected progressive uneven local subsidence and ground fissure activity at BCIA using time-series InSAR since 2010 [9].

Through a continuous monitoring period spanning 17 years, this study is dedicated to analyzing the long-term subsidence patterns of Beijing Capital International Airport (BCIA) and delving into the influencing factors and evolutionary trends of ground subsidence. Employing time-series InSAR (Interferometric Synthetic Aperture Radar) techniques to process multi-source SAR data from 2003 to 2023, we initially utilized data from ENVISAT ASAR, Cosmo-SkyMed, and Sentinel-1 to reveal the spatiotemporal characteristics of BCIA ground subsidence. Subsequently, a cross-validation with leveling measurement data was conducted to assess the precision of InSAR measurements. Ultimately, an in-depth analysis was performed on the current subsidence evolution and surface deformation of BCIA, accompanied by discussions on the relationships among ground subsidence, groundwater levels, and fault activities. The structure of the research is outlined with Section 2 providing an overview of the study area and the utilized datasets, Section 3 elucidating the theoretical foundation of InSAR and presenting the accuracy verification of the time-series InSAR results, Section 4 analyzing the spatiotemporal characteristics of BCIA ground subsidence, Section 5 discussing the relationships among ground subsidence, groundwater, and fault activities, and the analysis and discussion of subsidence evolution, followed by Section 6 summarizing the research findings.

The innovation of this study lies in offering a fresh perspective on ground changes in airport regions. Through an extended period of continuous monitoring of the Beijing Capital International Airport area, we have bridged gaps in prior research, providing robust data support for an in-depth analysis of the historical subsidence in airport regions. The noteworthy aspect of our work is the prolonged monitoring using a time-series approach, which serves as a key means to comprehensively and profoundly understand the geological evolution of airport areas. Additionally, our focus extends beyond surface deformation to a thorough analysis of the relationship between subsidence acceleration changes and the depth of groundwater. This exploration is crucial for predicting future trends in ground subsidence. By emphasizing observed surface rebound phenomena in the Chao Bai River replenishment area from previous studies, we underscore the close relationship between subsidence and groundwater levels.

Through this detailed analysis, we propose a potential transition from “stable subsidence” to “slow uplift” in future ground subsidence, providing substantial scientific evidence for subsequent control measures in groundwater replenishment.

2. Study Area and Data Sources

2.1. Study Area

BCIA is situated in the northeastern suburbs of Beijing, China, as illustrated in Figure 1. It is positioned 25 km southwest of the central city and was initially established in 1958. The airport covers an expansive area of 1.41 million square kilometers. In the year 1980, Terminal 1 (T1) was completed, including supporting facilities such as aprons, parking lots, and taxiways. On 1 November 1999, Terminal 2 (T2) commenced operations, leading to the temporary closure and renovation of T1. In September 2004, T1 was reactivated, and Terminal 3 (T3) was completed in 2008, with T1 undergoing refurbishment. BCIA boasts three runways, and notably, the central runway intersects a significant fault at an angle of 60 to 70 degrees toward the southeast. This fault, known as the SL Fault, exhibits vigorous activity primarily at its northern end. It formed due to tectonic activity in Beijing, traversing the runways of the airport.

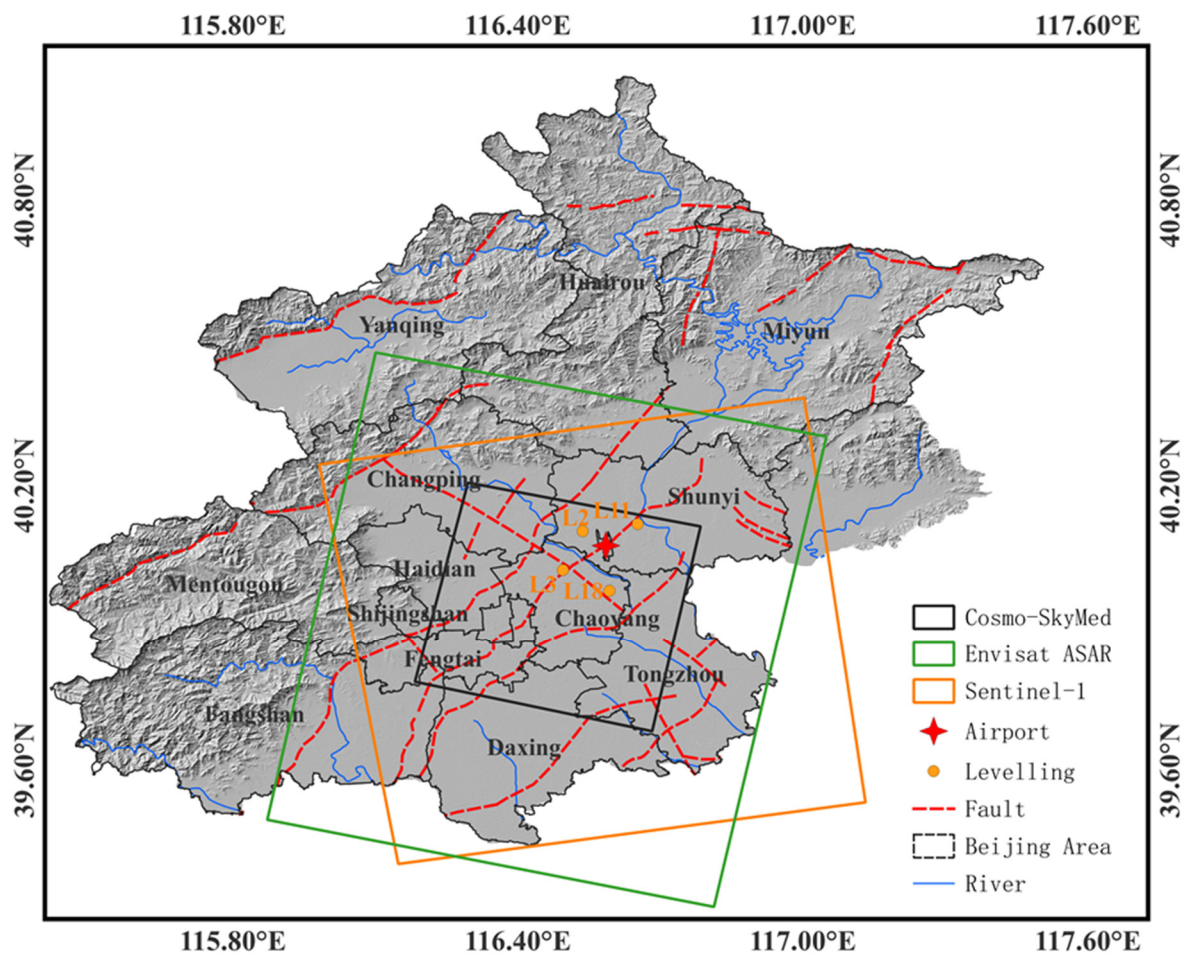


Figure 1. Research Area and Data Coverage Diagram.

2.2. Data Sources

1. InSAR Data

To conduct prolonged observations of BCIA, we curated a multi-sensor InSAR dataset, specifically designed for land subsidence monitoring. The dataset encompasses C-band ENVISAT ASAR data from 18 June 2003, to 16 June 2010, X-band Cosmo-SkyMed data

collected between 23 January 2013, and 3 August 2019, and C-band Sentinel-1 data spanning from 2 August 2019, to 14 March 2023. The essential details of the SAR data are presented in Table 1 below.

Table 1. SAR datasets parameters.

SAR Sensor	Mode	Time Series (Start/End)	Number of Acquisitions	Direction	Median Incidence Angle
ENVISAT-ASAR	IMS	18 June 2003 16 June 2010	52	Descending	22.8
Cosmo-SkyMed	IMS	23 January 2013 3 August 2019	67	Descending	19.3
Sentinel-1	IW	2 August 2019 14 March 2023	124	Ascending	42.3

2. Water Resources

Statistical data concerning groundwater levels, water supply, and water usage is provided by the Beijing Water Resources Bulletin. This encompasses metrics such as precipitation, surface water volume, groundwater volume, total water resources, water supply, and water usage. Information regarding groundwater depth, groundwater storage, water supply conditions, and factors like groundwater levels and the SNWDP are encompassed.

3. Leveling Data

To validate the accuracy of InSAR results, we collected leveling data from 13 continuous monitoring stations in the Beijing region. Notably, stations 2, 3, 11, and 18 served as the ground monitoring benchmarks, facilitating the accuracy validation of SAR data outcomes. The distribution of leveling stations is visualized in Figure 1.

3. Methodology

3.1. IPTA Method

Interferometric Point Target Analysis (IPTA) is a method that exploits the temporal and spatial characteristics of interferometric signatures collected from point targets that exhibit long-term coherence to map surface deformation. Use of the interferometric phase from long time series of data requires that the correlation remain high over the observation period [18,19].

Initially, the three types of Synthetic Aperture Radar (SAR) data were processed into Single Looking Complex (SLC) data. Each dataset was then subjected to coregistration to establish a consistent geometric pattern. For each registered dataset, the combination of the Amplitude Deviation Threshold method and Spectral Diversity was employed to identify Permanent Scatterer (PS) points. This process generated an interferogram stack of PS candidate points. Subsequently, after PS points were identified and phase extraction was accomplished, a linear deformation model was assumed at this stage. A linear regression analysis was performed for all points using a reference point, acquiring elevation correction values. Unwrapping of residual phases from linear regression was conducted, followed by baseline estimation, once the unwrapped phase integrity was confirmed. The atmospheric trend to the phase was estimated via spatiotemporal domain filtering, and this component was subtracted from the interferometric phase. Finally, through an iterative process, the deformation model was refined and its estimation was improved using estimates for atmospheric phase, deformation phase, elevation correction, and baseline phase, which were separated.

3.2. InSAR Results

Utilizing the IPTA technique, the surface deformation rate along the Line of Sight (LOS) in three types of SAR data were extracted, as illustrated in Figure 2. A uniform color scheme was applied to represent the deformation values, where positive values indicate movement towards the satellite and negative values signify movement away

from it, corresponding to downward ground motion. The results from all three datasets consistently revealed significant subsidence occurring at BCIA from 2003 to 2023. The subsidence was predominantly concentrated in the northern and western regions, consistent with prior InSAR studies [9,17].

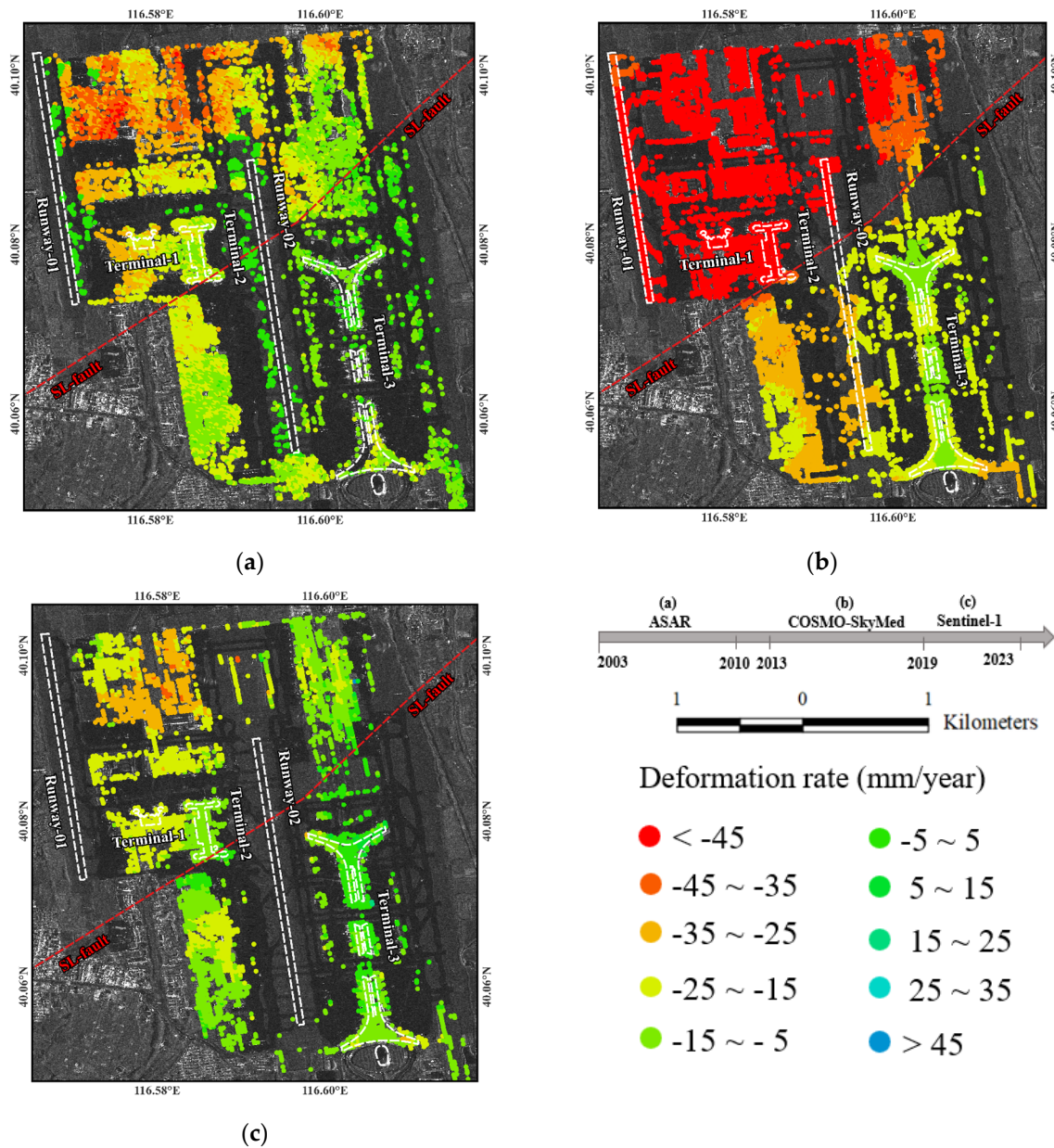


Figure 2. Land Subsidence Rate Map; (a) ENVISAT ASAR data from 18 June 2003, to 16 June 2010. Top right; (b) Cosmo-SkyMed data from 23 January 2013, to 3 August 2019; (c) Sentinel-1 date from 2 August 2019, to 14 March 2023.

The color-coded deformation rate map effectively captured intricate details of the airport's deformation. In Figure 2, the majority of the scatterer points were distributed over buildings, with sparser distribution over smoother runways and areas lacking angular reflective structures. The most heavily affected structures were Terminals 1 and 2 (T1 and T2), along with their respective Runway 1 and Runway 2. The cumulative subsidence for T1 and T2 was approximately 400 mm. It's important to note that although the scatterer distribution on Runway 2 appeared sparse, an analysis of the overall subsidence pattern indicates significant subsidence in the northern portion of Runway 2 while the southern

part remained stable. This suggests a prolonged non-uniform subsidence along Runway 2. Detailed information regarding non-uniform subsidence along the fault will be elaborated on in the following section.

From Figure 2, it is evident that Cosmo-SkyMed data detects higher subsidence rates at the airport, followed by Envisat ASAR and Sentinel-1. In the spatial distribution pattern of subsidence, distinct linear boundaries of subsidence can be observed. On either side of these linear boundaries, noticeable differential subsidence is identifiable. This boundary aligns well with the spatial extent of the subsidence caused by the SL Fault, indicating a significant overlap. It implies that the non-uniform subsidence at the airport is primarily influenced by this fault zone, with significantly higher subsidence rates on the northern side of the fault zone compared to its southern counterpart. The fault traverses through T2 and T3 runways as well as the T2 terminal.

3.3. Comparison of Leveling and InSAR Results

Various methods can be employed to verify InSAR deformation results, including GNSS, leveling, ground fissure meters, and field surveys. In the context of land subsidence, vertical deformation served as the principal component, and for InSAR accuracy assessment, we disregarded the impact of horizontal deformation. In previous studies, leveling monitoring results have often been used as effective validation data for InSAR monitoring outcomes. Effective InSAR observations can yield subsidence evolution values consistent with concurrent ground-based monitoring [20–23]. To ensure stability and consistency in comparative analysis, we initially selected four leveling points (point 2, point 3, point 11, and point 18) around the airport for a comparative analysis against InSAR results. Furthermore, it should be noted that there existed a data gap in InSAR monitoring data between 2011 and 2012, resulting in the absence of a single, continuous time series dataset to cover the entire study duration. To address it, we used the adjacent annual average deformation values to represent the deformation for these two missing years and calculated the deformation values for 2011 and 2012 using the average of deformation values from 2010, 2011, and 2013. Consequently, by combining available data, we cross-validated the annual InSAR subsidence values with leveling measurements to assess the quality of InSAR results. Figure 3 illustrates the temporal deformation sequences for the four leveling points and InSAR points. It can be observed from the graph that the two distinct observation methods exhibit a high level of agreement. According to the data, the correlation coefficient between the leveling observations at four points around the airport and the InSAR observations is 0.978. This indicates a strong positive correlation between the two sets of data. The root mean square errors for points 2, 3, 11, and 18 are 14.45 mm, 18.6 mm, and 14.45 mm, respectively. Comparative analysis with previous studies at the Capital Airport indicates that the deformation results obtained in this study exhibit consistency in spatial distribution with existing research outcomes. Deviations observed in the leveling and InSAR accuracy comparison analysis may be attributed to discrepancies in the positions or dates between InSAR deformation points and leveling points. Additionally, the presence of data gaps in this study could also contribute to this issue [9,17]. The results above indicate that the InSAR data processing method employed in this study is reliable and meets the accuracy requirements for ground deformation monitoring.

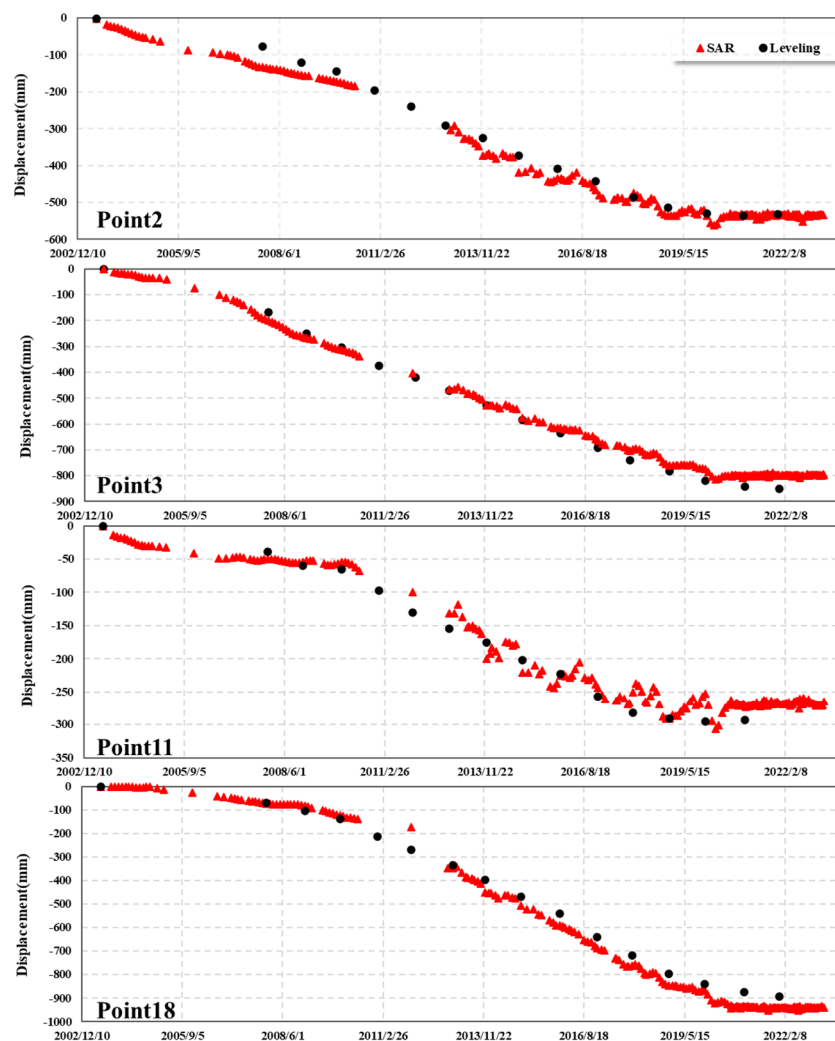


Figure 3. Accuracy Comparative Analysis of the Measurement Results of InSAR and Leveling.

4. Airport Subsidence Situation

As illustrated in Figure 2, the subsidence at BCIA exhibited distinct zoning characteristics as shown by the three types of SAR data. The deformation disparities between the northwest and southeast directions were substantial. Uneven subsidence had been occurring at the airport for multiple years and in regions with notable differences in deformation rates, surface damage phenomena should be more pronounced. These could include phenomena such as damage to artificially hardened surfaces, buildings, pipelines, and more. To trace the impact of uneven subsidence on the airport and facilitate a more direct assessment of surface damage within uneven subsidence areas, we collected optical images with a resolution of 0.2 m from 2010 to 2021.

Observing the yearly optical images of the airport, it becomes evident that significant ground fissures began appearing around 2010, accompanied by noticeable damage to the concrete surfaces. As depicted in Figure 4, noticeable cracks emerged on the south side and northeastern lawn of Terminal 2 in 2010. The concrete damage on the south side of the terminal was distinct, with visible ground cracks. By 2015, optical images displayed further expansion of ground fissures, and the concrete damage on the south side of Terminal 2 had worsened. The fissures extended from west to east, and a significant repair effort was undertaken at the junction of the northeastern runway patch Region I. This repair work was still visible in the 2020 imagery, differing from 2015. Notably, in the 2020 and 2021 images, repairs were observed on the east and south sides of Terminal 2 in patch Regions II and III, respectively.

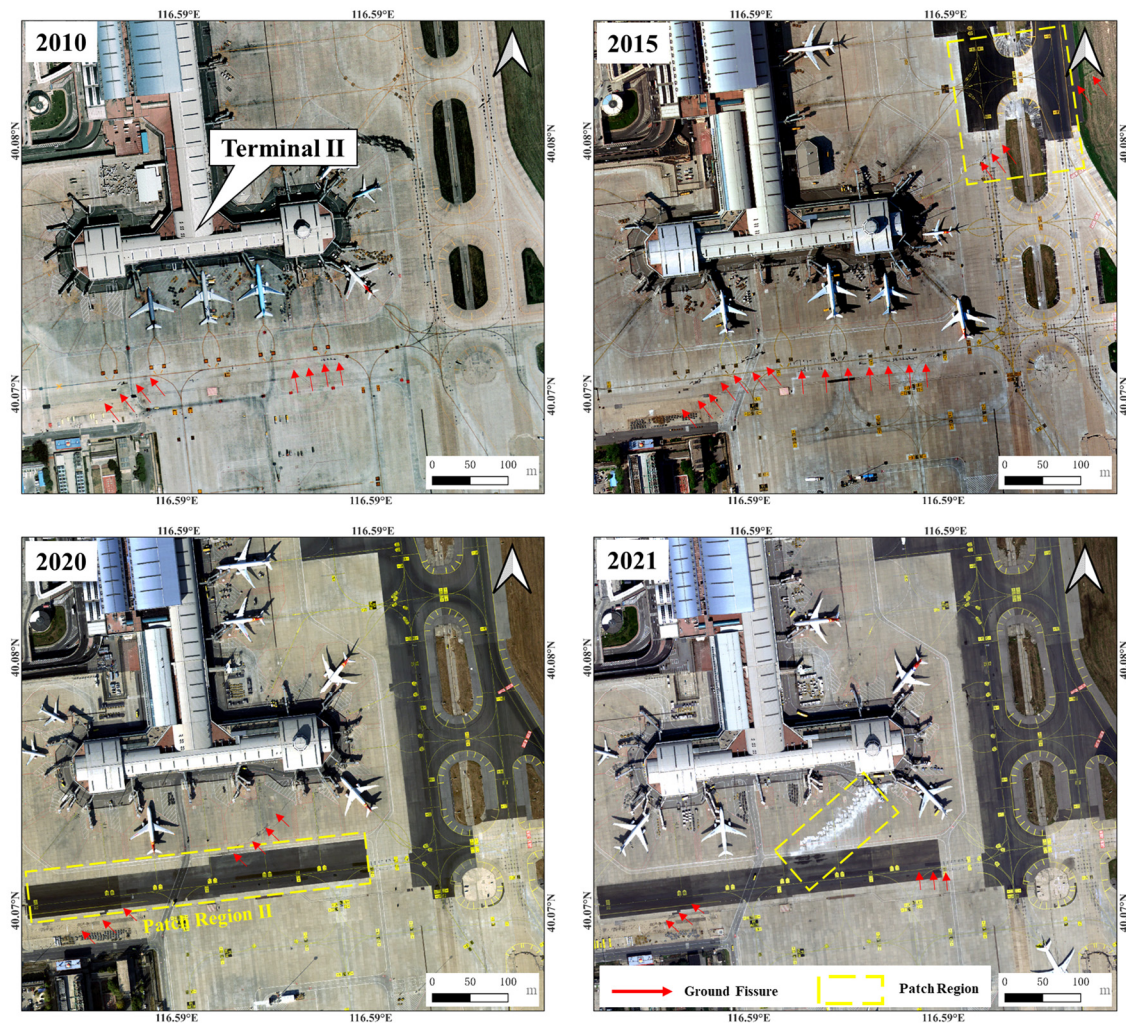


Figure 4. Illustration of Ground Fissures at BCIA in 2010, 2015, 2020, and 2021.

5. Discussion

5.1. Fault Zones and Ground Fissures

Due to the unique nature of the airport environment, immediate physical explorations or other relevant activities were not available during the research process. We collected existing geological data and overlaid it with the deformation rate map. The SL Fault, a significant active fault in the Holocene era, is closely related to geological safety concerns such as ground fissures and differential land subsidence in Beijing. As previously mentioned, the subsidence at the airport exhibited distinct zoning characteristics, with substantial deformation disparities on either side of the fault. The uneven subsidence has persisted for nearly 20 years, from 2003 to 2023. The intersection between the airport runways and the SL fault is evident in the analysis of the InSAR deformation rate map. The land subsidence is notably influenced by fault activity. The northwest part of the airport experienced more pronounced subsidence, with the SL fault marking the subsidence boundary and forming a clear demarcation line in deformation on either side of the fault.

To clearly identify the differential subsidence on either side of the fault, the study plotted the results from the period of significant subsidence from 2013 to 2019 using Cosmo-SkyMed data. As shown in Figure 5, the deformation values of scatterers across the entire airport are distributed in two distinct layers concerning distance. The maximum subsidence on the northwest side of the fault is -494.25 mm, with an average subsidence value of -442.2 mm and a subsidence rate of 73.7 mm/year. On the southeast side of the fault, the minimum subsidence is -45.8 mm, with an average subsidence value of -131.2 mm and a

subsidence rate of 21.8 mm/year. The maximum difference in relative position between the two sides of the fault zone is 448.45 mm, with differences in subsidence rates and average subsidence rates of 51.9 mm and 311 mm, respectively.

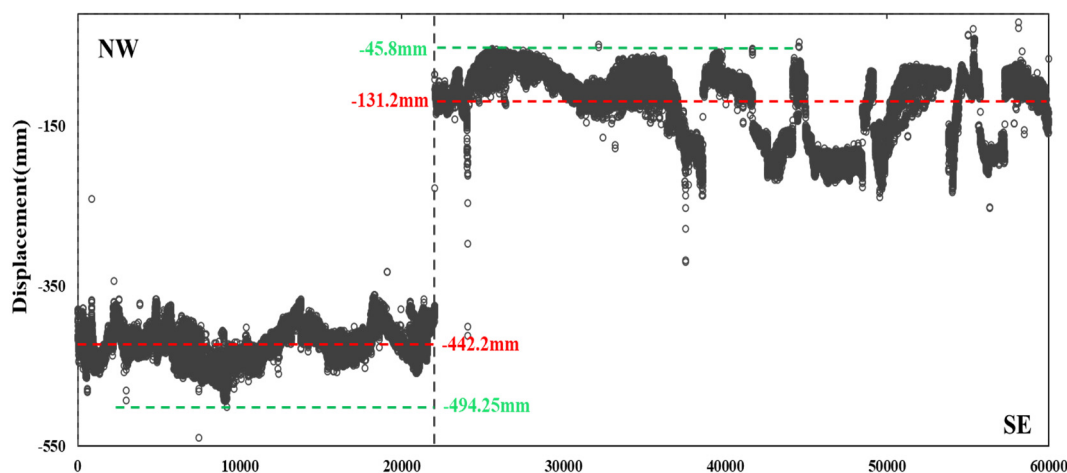


Figure 5. Distribution of Land Subsidence Displacements on Both Sides of the SL Fault in the BCIA Area.

The uneven land subsidence reflected in the InSAR results provides clues for the occurrence of ground fissures at the airport. The distribution of ground fissures shown in Figure 4 is situated around the fault zone, and the intensified differential subsidence on either side of the fault has exacerbated surface damage occurrences.

5.2. Groundwater

In the Beijing plain area, widespread subsidence has occurred in the eastern part, including areas like Chaoyang, Tongzhou, and northeastern Haidian, where the subsidence rate exceeds 100 mm/year [10]. Previous research indicated that the subsidence in the Beijing region was primarily caused by extensive groundwater extraction and the presence of compressible subsurface sediments in the plain contributed to land subsidence [11,13,24]. As shown in Figure 6, to better illustrate the correlation between deformation at the airport and groundwater, we conducted a correlation analysis between four characteristic points around the airport and the average groundwater level depth in the plain. The groundwater level data were obtained from the “Beijing Water Resources Bulletin” published by the Beijing Water Authority.

From the four characteristic points, it can be observed that between 2003 and 2010, the land slowly subsided. During this period, the groundwater level progressively decreased, showing a good consistency between subsidence and variations in groundwater depth.

Between 2010 and 2018, the land subsidence rate increased further. During this period, the groundwater level variations in the plain were relatively small, with a significant drop in groundwater depth only observed from 2014 to 2016. According to related literature, after the completion of the first phase of the SNWDP in 2008, the groundwater supply in Beijing progressively decreased, leading to a reduction in groundwater extraction. Consequently, the groundwater level variations were smaller compared to the earlier period before 2008. With the implementation of the second phase of the SNWDP in 2015, the groundwater supply in 2021 had decreased by 50.3% and 40.04% compared to the years 2000 and 2008, respectively. The use of diverted water for reservoir and river ecological restoration, as well as groundwater replenishment, effectively facilitated the recovery of severely exploited groundwater areas. By 2015, the groundwater level had rebounded by 3.45 m, from 25.75 m to 22.3 m.

From 2016 to 2020, the groundwater level rose continuously, resulting in a noticeable deceleration of land subsidence. The subsidence values at the four characteristic points gradually decreased after 2016. Although still undergoing subsidence, the rate significantly

slowed compared to the period before 2016. For instance, characteristic point 11 exhibited a deformation value of -252.448 mm in 2018, -290.548 mm in 2019, and uplifted by 38.1 mm in ground elevation. Points 2 and 3 experienced stable subsidence around 2022. Thus, groundwater level changes are a significant factor influencing subsidence in the airport area, exhibiting a strong correlation over long-time series evolution. However, in certain years, we found slight discrepancies between groundwater variations and land subsidence. For example, at point 18, deformation continued to accelerate between 2018 and 2020. This divergence might be attributed to distinct hydrogeological characteristics or spatial properties of geological sediments in different areas.

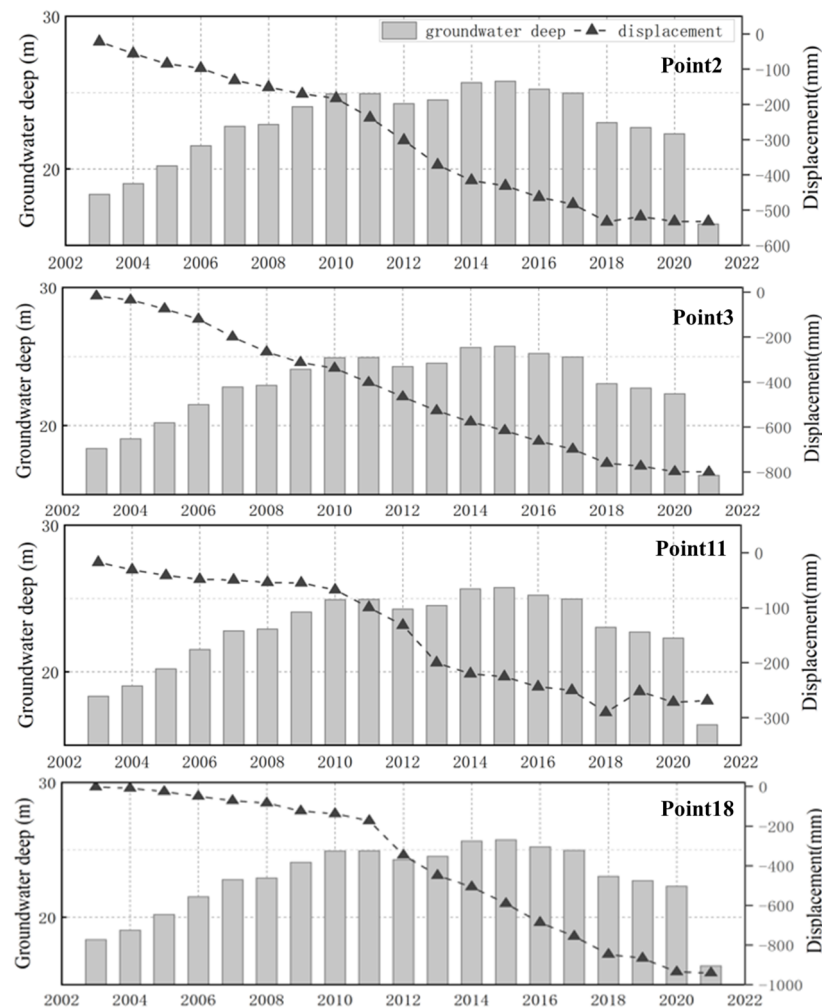


Figure 6. Correlation Illustration between Groundwater Depth and Surface Deformation in BCIA.

5.3. Analysis of Subsidence Evolution

The preceding analysis of InSAR results examined the subsidence of BCIA. The findings indicated that subsidence accelerated before 2016, with spatial development influenced by fault lines and groundwater level variations serving as the primary driving factor. On this basis, we delved into the evolving patterns of subsidence at the airport.

The subsidence at BCIA occurs within the subsidence cone of the Beijing Plain. In recent years, the city has undertaken reforms in water supply and usage structures, leading to a reduction in groundwater extraction. Additionally, a portion of the SNWDP water is directed to water treatment plants, addressing the city's water demands. Another portion is stored in infiltration reservoirs to replenish the aquifer system. The groundwater replenishment pathway for the Beijing Plain is located at the confluence of the Chaobai River and the Huai River. Based on the analysis of temporal subsidence changes in the

preceding sections, the subsidence of the airport gradually slowed down in the later stages of 2016. It remains uncertain whether the future will witness a shift from “stable subsidence” to “slow uplift.” Nevertheless, it’s noteworthy that soil layers that shrink due to loss of water during declining groundwater levels tend to expand upon water absorption during rising groundwater levels, leading to a certain degree of ground rebound. The results depicted in Figure 7 intuitively illustrate the spatiotemporal dynamics of subsidence acceleration and groundwater depth variations at four different reference points around the airport. The data spans from 2003 to 2021, providing a comprehensive temporal framework for analysis. During phases where subsidence acceleration is greater than zero, the uplifting pressure exerted by the subsurface layers on the surface exceeds the accumulated downward pressure. Consequently, the total force within the subsidence area counteracts the subsidence movement. Conversely, negative acceleration phases indicate that the cumulative uplifting pressure from the subsurface layers is smaller than the combined downward supporting forces. Therefore, the overall direction of ground forces aligns with subsidence movement within the subsidence area. It is noteworthy that after 2012, the acceleration values at the four characteristic points gradually increased. Around 2015, all characteristic points exhibited positive acceleration values. This signifies a shift in the ground force vector direction around the Capital Airport, transitioning from the existing downward pressure to primarily upward supporting forces. Starting from 2015, the average depth of groundwater in the plain area gradually decreased, and the groundwater level began to rise. The established relationship between the accelerated subsidence rate and groundwater depth confirms their highly correlated and mutually constraining nature.

However, a specific condition exists: when the groundwater level rises, soil layers that previously contracted due to water loss will reabsorb water, causing the ground to experience a rebound effect. In the study, it was observed that, although there was a noticeable deceleration in acceleration after 2018 at all four characteristic points, the acceleration values at these points remained greater than zero. This indicates that the uplifting pressure exerted by the subsurface layers on the surface still exceeded the accumulated downward pressure. Therefore, prolonged accumulation can lead to ground uplift. Moreover, in the area of water supplementation through the Chaobai River, significant rebound phenomena have already been observed [16], though widespread surface uplift has yet to manifest.

The rebound of subsidence correlates strongly with the sustained recovery of groundwater levels. The question of whether the airport area’s subsidence could transition into an uplift in the future, along with predicting the magnitude of this uplift, holds significant implications. If ground uplift occurs, infrastructure within the airport premises and underground pipelines may experience uneven tension or compression, potentially resulting in ground fractures, breaks, or shifts that could impact airport operations. The decisive factor in ground uplift lies in whether the previously compacted soil undergoes a rebound following water replenishment after groundwater level recovery. Concerning the variation in groundwater storage in the Beijing Plain and future predictions, Long et al. [25] conducted simulated analyses for the period between 2019 and 2030, considering precipitation and groundwater extraction scenarios. Their findings indicate that by 2030, groundwater levels are expected to return to approximately the same depth as in 2003, around -18 m. While groundwater storage may significantly recover in the next decade, the consolidative characteristics of clay layers in the airport area will play a pivotal role in determining whether ground uplift occurs.

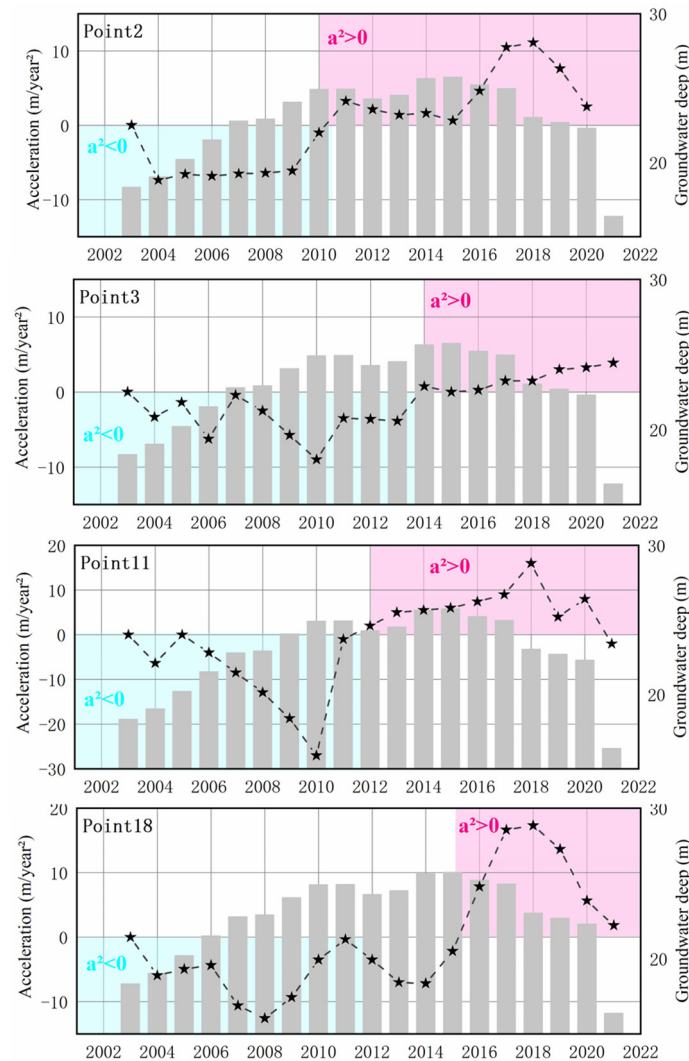


Figure 7. Correlation diagram of deformation acceleration at characteristic points of Capital Airport and depth of groundwater level.

6. Conclusions

This study conducted an in-depth investigation into the long-term ground displacement of Beijing Capital International Airport (BCIA) using time-series InSAR technology. During the survey period from 18 June 2003, to 14 March 2023, the IPTA time-series method was applied to analyze three sets of SAR data, resulting in comprehensive time-series monitoring outcomes. Observations revealed a significant subsidence in the airport area over the past 20 years. In comparison to leveling measurement results, the subsidence trend monitored by InSAR exhibited remarkable consistency, demonstrating a high level of overall agreement. Time-series analysis indicated that the subsidence at BCIA primarily occurred along the boundary of the SL fault, with noticeable differences in subsidence on either side of this boundary. The formation of surface cracks was concentrated in areas with subsidence disparities.

Excessive groundwater extraction is considered the principal factor contributing to ground subsidence. Initially, influenced by both groundwater extraction and the natural consolidation of sediments, a subsidence funnel takes shape. Nevertheless, the presence of the SL fault interrupts the subsidence, causing it to spread on either side of the fault. Subsequently, the subsidence accumulates gradually, leading to surface differential deformation, where the concrete subsidence rate is higher in the lower layer than in the upper layer. Consequently, bending and localized uplift occur at the periphery of the concrete surface

subsidence basin. Given the special environmental conditions and the presence of ground faults around the airport, we recommend integrating satellite-based InSAR technology with ground surveys to monitor and predict ground fault activity, ensuring technical support for airport operations. This highlights the applicability of InSAR technology in identifying and monitoring ground subsidence, ground fault activity, and other geological processes, providing a scientific approach to explore the causes and mechanisms of subsidence and ground faults in the region.

This study lies in providing a new perspective on ground changes in airport areas. Through continuous monitoring of the Beijing Capital International Airport area over a long time series, we have filled knowledge gaps in previous research and provided robust data support for in-depth analysis of historical subsidence in the airport area. The extended time-series monitoring is a major highlight of our work, offering essential means to comprehensively and deeply understand the geological evolution of the airport area. Additionally, our focus extends beyond surface deformation to a thorough analysis of the relationship between subsidence acceleration and groundwater depth. The discussion of this relationship is crucial for predicting the future trends of ground subsidence. By pointing out the observed surface rebound phenomenon in the Chao Bai River replenishment area in previous studies, we emphasize the close relationship between subsidence and groundwater levels. Through in-depth analysis, we propose a potential transition from “stable subsidence” to “slow rise” in future ground subsidence, providing a substantial scientific basis for subsequent groundwater replenishment regulation.

Author Contributions: Conceptualization, Y.Z. and J.P.; methodology, Y.Z.; software, X.C. and X.M.; validation, C.L. and Y.P.; formal analysis, M.H.; All authors have read and agreed to the published version of the manuscript.

Funding: This research was funded by The National Natural Science Foundation of China (Grant Nos. 42074004), research grants from National Institute of Natural Hazards, Ministry of Emergency Management of China (Grant Nos. ZDJ2022). The Third Xinjiang Scientific Expedition and Research Program (Grant No. 2022xjkk0600); The Second Tibetan Plateau Scientific Expedition and Research Program (STEP) (Grant No. 2019QZKK0904); Funding: This research was funded by Beijing Key Laboratory of Urban Spatial Information Engineering (No. 20220102).

Data Availability Statement: The publicly available C-band ENVISAT-ASAR data is sourced from <https://eocat.esa.int/sec/#data-services-area> (accessed on 19 January 2024), C-band Sentinel data is obtained from <https://eocat.esa.int/sec/#data-services-area> (accessed on 19 January 2024), and water level data is sourced from <https://swj.beijing.gov.cn/> (accessed on 19 January 2024).

Conflicts of Interest: Author Yun Peng was employed by the company Power China Zhongnan Engineering Corporation Limited, 16 Xiangzhang East Road, Changsha 410014, Yuhua District. The remaining authors declare that the research was conducted in the absence of any commercial or financial relationships that could be construed as a potential conflict of interest. The company Power China Zhongnan Engineering Corporation Limited in affiliation and funding had no role in the design of the study, in the collection, analyses, or interpretation of data, in the writing of the manuscript, or in the decision to publish the results.

References

1. Kuenzer, C. Detecting and Analyzing the Evolution of Subsidence Due to Coal Fires in Jharia Coalfield, India Using Sentinel-1 SAR Data. *Remote Sens.* **2021**, *13*, 1521.
2. Fernandez, J.; Prieto, J.F.; Escayo, J.; Camacho, A.G.; Luzón, F.; Tiampo, K.F.; Palano, M.; Abajo, T.; Pérez, E.; Velasco, J. Modeling the two- and three-dimensional displacement field in Lorca, Spain, subsidence and the global implications. *Sci. Rep.* **2018**, *8*, 14782. [[CrossRef](#)] [[PubMed](#)]
3. Ortega-Guerrero, A.; Rudolph, D.L.; Cherry, J.A. Analysis of long term land subsidence near Mexico City: Field investigations and predictive modelling. *Water Resour. Res.* **1999**, *35*, 3327–3341. [[CrossRef](#)]
4. Sun, H.; Grandstaff, D.; Shagam, R. Land subsidence due to groundwater withdrawal: Potential damage of subsidence and sea level rise in southern New Jersey, USA. *Environ. Geol.* **1999**, *37*, 290–296. [[CrossRef](#)]
5. Nasiri, A.; Shafiei, N.; Kia, R.F. Investigation of Fahlian aquifer subsidence and its effect on groundwater loss. *Arab. J. Geosci.* **2021**, *14*, 637. [[CrossRef](#)]

6. Aobpaet, A.; Cuenca, M.C.; Hooper, A.; Trisirisatayawong, I. Land subsidence evaluation using insar time series analysis in bangkok metropolitan area. In Proceedings of the Fringe 2009 Workshop, Frascati, Italy, 30 November–4 December 2009.
7. Yamanaka, T.; Mikita, M.; Lorphensri, O.; Shimada, J.; Kagabu, M.; Ikawa, R.; Nakamura, T.; Tsujimura, M. Anthropogenic changes in a confined groundwater flow system in the Bangkok Basin, Thailand, part II: How much water has been renewed? *Hydrol. Process.* **2011**, *25*, 2734–2741. [[CrossRef](#)]
8. Yastika, P.E.; Shimizu, N.; Abidin, H.Z. Monitoring of long-term land subsidence from 2003 to 2017 in coastal area of Semarang, Indonesia by SBAS DInSAR analyses using Envisat-ASAR, ALOS-PALSAR, and Sentinel-1A SAR data. *Adv. Space Res.* **2019**, *63*, 1719–1736. [[CrossRef](#)]
9. Gao, M.; Gong, H.; Li, X.; Chen, B.; Zhou, C.; Shi, M.; Guo, L.; Chen, Z.; Ni, Z.; Duan, G. Land Subsidence and Ground Fissures in Beijing Capital International Airport (BCIA): Evidence from Quasi-PS InSAR Analysis. *Remote Sens.* **2019**, *11*, 1466. [[CrossRef](#)]
10. Zheng, Y.; Peng, J.; Chen, X.; Huang, C.; Chen, P.; Li, S.; Su, Y. Spatial and Temporal Evolution of Ground Subsidence in the Beijing Plain Area Using Long Time Series Interferometry. *IEEE J. Sel. Top. Appl. Earth Obs. Remote Sens.* **2022**, *16*, 153–165. [[CrossRef](#)]
11. Chen, M.; Tomás, R.; Li, Z.; Motagh, M.; Li, T.; Hu, L.; Gong, H.; Li, X.; Yu, J.; Gong, X. Imaging land subsidence induced by groundwater extraction in Beijing (China) using satellite radar interferometry. *Remote Sens.* **2016**, *8*, 468. [[CrossRef](#)]
12. Simons, M.; Rosen, P.A. Interferometric Synthetic Aperture Radar Geodesy. *Treatise Geophys.* **2007**, *3*, 339–385.
13. Gong, H.; Pan, Y.; Zheng, L.; Li, X.; Zhu, L.; Zhang, C.; Huang, Z.; Li, Z.; Wang, H.; Zhou, C. Long-term groundwater storage changes and land subsidence development in the North China Plain (1971–2015). *Hydrogeol. J.* **2018**, *26*, 1417–1427. [[CrossRef](#)]
14. Hu, L.; Dai, K.; Xing, C.; Li, Z.; Tomás, R.; Clark, B.; Shi, X.; Chen, M.; Zhang, R.; Qiu, Q.; et al. Land subsidence in Beijing and its relationship with geological faults revealed by Sentinel-1 InSAR observations. *Int. J. Appl. Earth Obs. Geoinf.* **2019**, *82*, 101886. [[CrossRef](#)]
15. Zhou, C.; Gong, H.; Chen, B.; Gao, M.; Cao, Q.; Cao, J.; Duan, L.; Zuo, J.; Shi, M. Land Subsidence Response to Different Land Use Types and Water Resource Utilization in Beijing-Tianjin-Hebei, China. *Remote Sens.* **2020**, *12*, 457. [[CrossRef](#)]
16. Dong, J.; Guo, S.; Wang, N.; Zhang, L.; Ge, D.; Liao, M.; Gong, J. Tri-decadal evolution of land subsidence in the Beijing Plain revealed by multi-epoch satellite InSAR observations. *Remote Sens. Environ.* **2023**, *286*, 113446. [[CrossRef](#)]
17. Dai, K.; Shi, X.; Gou, J.; Hu, L.; Chen, M.; Zhao, L.; Dong, X.; Li, Z. Diagnosing Subsidence Geohazard at Beijing Capital International Airport, from High-Resolution SAR Interferometry. *Sustainability* **2020**, *12*, 2269. [[CrossRef](#)]
18. Werner, C.; Wegmuller, U.; Wiesmann, A.; Strozzi, T. Interferometric Point Target Analysis with JERS-1 L-band SAR data. In Proceedings of the IGARSS 2003. 2003 IEEE International Geoscience and Remote Sensing Symposium, Toulouse, France, 21–25 July 2003. Proceedings (IEEE Cat. No. 03CH37477).
19. Zhang, Y.; Zhang, J.; Wu, H.; Lu, Z.; Guangtong, S. Monitoring of urban subsidence with SAR interferometric point target analysis: A case study in Suzhou, China. *Int. J. Appl. Earth Obs. Geoinf.* **2011**, *13*, 812–818. [[CrossRef](#)]
20. Serrano-Juan, A.; Pujades, E.; Vázquez-Suñer, E.; Crosetto, M.; Cuevas-González, M. Leveling vs. InSAR in urban underground construction monitoring: Pros and cons. Case of la sagrera railway station (Barcelona, Spain). *Eng. Geol.* **2016**, *218*, 1–11. [[CrossRef](#)]
21. Chen, J.; Zhou, Y.; Chen, G.; Hao, M. Decades of Ground Deformation in the Weihe Graben, Shaanxi Province, China, in Response to Various Land Processes, Observed by Radar Interferometry and Levelling. *Remote Sens.* **2021**, *13*, 2374. [[CrossRef](#)]
22. Mingliang, G.; Huili, G.; Beibei, C.; Xiaojuan, L.; Chaofan, Z.; Min, S.; Yuan, S.; Zheng, C.; Guangyao, D. Regional Land Subsidence Analysis in Eastern Beijing Plain by InSAR Time Series and Wavelet Transforms. *Remote Sens.* **2018**, *10*, 365.
23. Chen, B.; Gong, H.; Chen, Y.; Li, X.; Zhao, X. Land subsidence and its relation with groundwater aquifers in Beijing Plain of China. *Sci. Total Environ.* **2020**, *735*, 139111. [[CrossRef](#)]
24. Du, Z.; Ge, L.; Ng, A.H.-M.; Lian, X.; Zhu, Q.; Horgan, F.G.; Zhang, Q. Analysis of the impact of the South-to-North water diversion project on water balance and land subsidence in Beijing, China between 2007 and 2020. *J. Hydrol.* **2021**, *603*, 126990. [[CrossRef](#)]
25. Long, D.; Yang, W.; Scanlon, B.R.; Zhao, J.; Liu, D.; Burek, P.; Pan, Y.; You, L.; Wada, Y. South-to-North Water Diversion stabilizing Beijing's groundwater levels. *Nat. Commun.* **2020**, *11*, 3665. [[CrossRef](#)]

Disclaimer/Publisher's Note: The statements, opinions and data contained in all publications are solely those of the individual author(s) and contributor(s) and not of MDPI and/or the editor(s). MDPI and/or the editor(s) disclaim responsibility for any injury to people or property resulting from any ideas, methods, instructions or products referred to in the content.